JOURNAL OF OPTOELECTRONICS AND ADVANCED MATERIALS Vol. 12, No. 3, March 2010, p. 466 - 469

Thermal budget considerations for excimer laser annealing of implanted dopants

V. GONDA[a], J. VENTURINI[b], C. SABATIER[b], J. VAN DER CINGEL[c], L. K. NANVER[c]
[a]*College of Dunaújváros, Táncsics M. u. 1/A, 2400 Dunaújváros, Hungary*
[b]*Excico, 13-21 quai des Grésillons, Bat. B7, 92230 Gennevilliers, France*
[c]*Delft University of Technology, DIMES-ECTM, Feldmannweg 17, 2628CD Delft, The Netherlands*

For activation of implanted dopants in bulk silicon with excimer laser annealing, the optimal laser energy density will depend on the substrate heating, and the pulse width and shape. These parameters will determine the thermal cycle and the heat affected zone. The latter is particularly important for low thermal budget annealing of electronic devices. In this work, two methods were studied, both based on XeCl excimer laser setups. Either a long pulse (180 ns) single laser setup by Excico was used, or a double laser setup with 25 ns native pulse width in DIMES. In the latter, the pulse shape and the temporal thermal profile can be tailored with short pulse offsets. This way the total thermal budget can be increased while the laser energy of each pulse is decreased, for the same sheet resistance. In this paper, the two methods are compared by sheet resistance measurements on laser annealed arsenic implants. The temporal and spatial thermal profiles were also calculated for both methods. Results show that the laser energy density can range from 600-1850 mJ/cm^2 to give full activation with different thermal profiles based upon the method used.

(Received June 30, 2009; accepted October 8, 2009)

Keywords: Excimer laser annealing, Double laser anneal, Pulse shape, Pulse duration, Thermal simulation

1. Introduction

Ultrashallow junctions with excellent electrical properties can be formed by excimer laser annealing of implanted dopants. In the melted and regrown region, very high dopant activation can be achieved with perfect crystalline quality. Moreover, the heat affected zone is very small, which makes this method applicable, where furnace annealing is not an option. This was shown for in conjunction with silicon-on-glass bipolar transistors [1], SiGe HBT [2], and high-k metal gate MISFET [3].

However, due to the extremely low thermal budget, significant implantation damage can remain below the melted and regrown region [4]. Nevertheless, for some applications the lowest thermal budget possible is required as it provides the shallowest heat affected zone. The critical depth for these devices is about 100 nm. Tailoring the thermal budget is not straightforward in melt laser annealing. In this work, two methods were studied, both based on XeCl excimer laser setups. Either a long pulse (180 ns) single laser setup by Excico [5] was used, or a double laser setup in DIMES. In the latter, the pulse shape and the temporal thermal profile were tailored with short pulse offsets in the range from 0 ns to 400 ns. In this paper, the two methods are compared by sheet resistance measurements on laser annealed arsenic implants. Computer simulations were used to estimate the thermal cycle for the silicon surface and in the 100 nm depth for both methods. Results show that the laser energy density can range from 600-1850 mJ/cm^2 to give full activation with different thermal profiles based upon the method used.

2. Experimental procedures

A double laser system and a long pulse laser system were used in the work. The schematic of the double laser system is shown in Figure 1. It consists of two Lambda physics XeCl laser sources emitting at 308 nm with a native pulse width of 25 ns measured at full width at half maximum (FWHM). The lasers can be ignited with pre-defined delays (pulse offsets) by the pulse generator. When 0 offset is used, then the two lasers are simultaneously ignited, however a time jitter can occur, which is about 4 ns at 1σ. The second laser system is a special long pulse XeCl system built by Excico, where the pulse width is 180 ns FWHM. The pulse shapes for the double laser system with 0 and 100 ns offset are shown in Fig. 2, together with the shape of the Excico's laser pulse. The samples were 4" diameter, 0.5 mm thick p-type wafers implanted with As^+ at 15 keV with a dose of 5 x 10^{14} cm^{-2}. Four laser anneals were made in vacuum as summarized in Table 1: a) substrate heated to 300 ^{o}C, 25 ns pulse, b) room temperature substrate with 25 ns pulse, c) room temperature substrate, double pulsed 2 x 25 ns pulse with 100 ns delay, and d) room temperature substrate with a single 180 ns pulse. The laser fluences were in the range from 500-3000 mJ/cm^2. Subsequently, the sheet resistance were measured with 4-point probe.

The thermal profiles were calculated with a 1-D model. The thermal properties of silicon were temperature dependent, the reflectivity was phase dependent, and the melting was incorporated into the model by the enthalpy method [6]. The governing equation considers transient heat conduction as:

$$\rho c^*(T)\frac{\partial T}{\partial t} = \frac{\partial}{\partial x}\left(k(T)\frac{\partial T}{\partial x}\right) + Q(x,t) \quad (1)$$

where ρ is the density of silicon, k is the thermal conductivity, T is the absolute temperature, t is time and x is the depth from the surface. The modified specific heat capacity, c^* is defined as:

$$c^*(T) = c(T) + L_H \delta(T - T_m) \quad (2)$$

where c is the specific heat capacity of silicon, L_H is the latent heat, and δ is the Dirac delta function, T_m is the melt temperature of silicon.

The laser energy absorbed by the silicon, Q, is defined as:

$$Q(x,t) = (1-R)I(t)\alpha\exp(-\alpha x) \quad (3)$$

where α is the absorption coefficient, R is the reflectivity of silicon, and I is the pulse intensity.

The boundary conditions are isolation at the surface and constant temperature at the bottom of the substrate:

$$\left.\frac{\partial T}{\partial x}\right|_{x=0} = 0;\ T_{xmax} = T_0 \quad (4)$$

The material properties are summarized in Table 2.

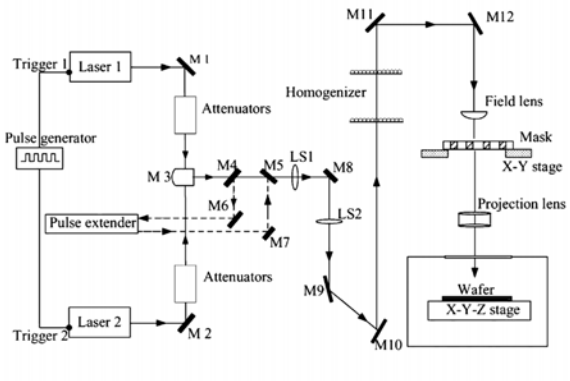

Fig. 1. Schematic of the double laser system.

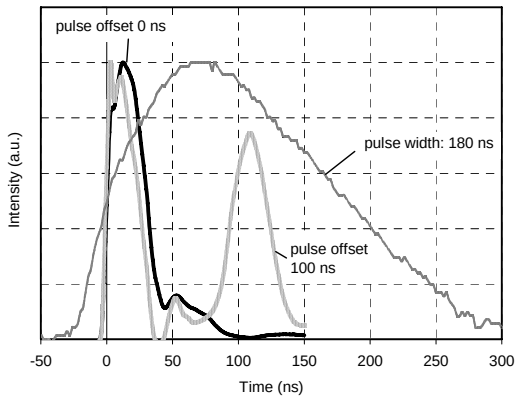

Fig. 2. Pulse shapes from the double laser system at 0 and 100 ns pulse offsets, and Excico's 180 ns pulse.

Table 1. Laser annealing parameters.

Case	Chuck temperature (°C)	Pulse width (ns)	Pulse delay (ns)
a	300	25	0
b	20	25	0
c	20	25	100
d	20	180	-

Table 2. Thermal and optical properties of silicon used in the simulation.

	Solid	Liquid
ρ [g/cm^3]	2.33	2.33
c [J/gK]	$0.81 + 1.3 \times 10^{-4}T - 1.26 \times 10^{4}T^{-2}$	1
k [W/cmK]	$0.235 + 4.45\exp(-T/247)$	$0.502 + 2.99 \times 10^{-4}(T-T_m)$
α [cm^{-1}]	10^6	10^6
R [-]	0.7	0.65
L_H [J/g]	1780	
T_m [K]	1687	

3. Results and discussions

Measured sheet resistances of the laser annealed As^+ at 15 keV, 5 x 10^{14} cm^{-2} implanted layer are shown in Fig. 3 for the different laser anneals as a function of the total laser energy density. In the double laser system each laser irradiates at the half of the total energy density. The sheet resistance, R_s is inversely proportional to electron charge, q, the active concentration N and the mobility μ:

$$R_s = \frac{1}{q\mu(x_m)N(x_m)x_m} \quad (5)$$

These parameters are strongly dependent on the melt depth, x_m, therefore the sheet resistance decreases with the increasing laser energy density as the melt depth increases. To reach a sheet resistance of 300 ohm/sq, a total fluence of 600, 800, 1200 and 1850 mJ/cm^2 is needed for the different laser anneals summarized in Table 1. By using the double laser system, increasing pulse offsets will shift the sheet resistance curves towards higher energies, while the chuck or substrate heating will shift the curve towards lower energies with respect to the anneal with no offset at room temperature. As pulse offsets above 100 ns are less effective [7], the fluence range for this particular implant can be tailored from 600-1200 mJ/cm^2. Further increasing the fluence for the same sheet resistance is only possible by increasing the laser pulse width. The results for an anneal with a 180 ns pulse is shown in Figure 3 with a dashed line. As the pulse width increases, the maximal intensity decreases and the thermal gradients decreased too. The reduced solid/liquid interface velocity may influence the segregation processes [8]. These are beneficial for defect anneal and to avoid ablation [5].

The thermal profiles were simulated for these anneals at a total fluence of 600, 800, 1200 and 1850 mJ/cm^2,

respectively. The surface temperature and the temperature at 100 nm depth are shown in Figure 4 for each case. The maximum melt depth was 50 nm in each case, and the depth of 100 nm was chosen because it is a critical depth for the devices mentioned in the introduction. In general, the thermal cycles that are induced by the laser pulse are much longer than the laser pulse itself, the temperature decay elongates the thermal cycle. In zero offset and the single shot anneals, the melt and regrowth, that is the complete anneal occurs by pulse. In the double pulsed anneals with pulse pairs, melting might not reached at the first pulse, but as the second pulse arrives when the cooling is not completed, it has a temperature advantage, similarly as the case of the heated substrate. It is also seen that the time in the melt is slightly different for the different anneals. Moreover the temperature difference between the surface and in the depth is different during the melting, while this difference vanished during cooling.

The temperature difference between 50 and 100 nm depth as a function of time for the different laser anneals is shown in Fig. 5. As the melt depth reaches 50 nm, the maximum temperature can just reach the melt temperature of crystalline silicon, but not exceed it. For the ultra shallow anneals and tight thermal limitations this difference should be large, while for defect anneal, and deep recrystallization this difference should be low. The extents of these anneals are the short and long pulse anneals, the long pulse anneal results 100 ^{o}C higher temperature at 100 nm depth than the short pulse anneal.

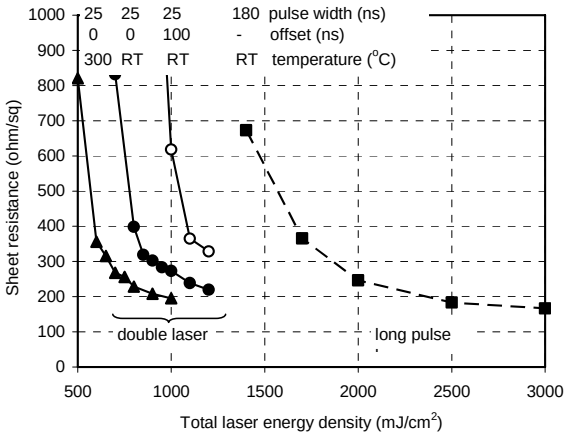

Fig. 3. Measured sheet resistance of the As^{+} at 15 keV, 5 x 10^{14} cm^{-2} implanted layer as a function of the laser energy density, laser annealed with a substrate at room temperature or 300 ^{o}C, pulse width of 25 or 180 ns, single or double pulsed.

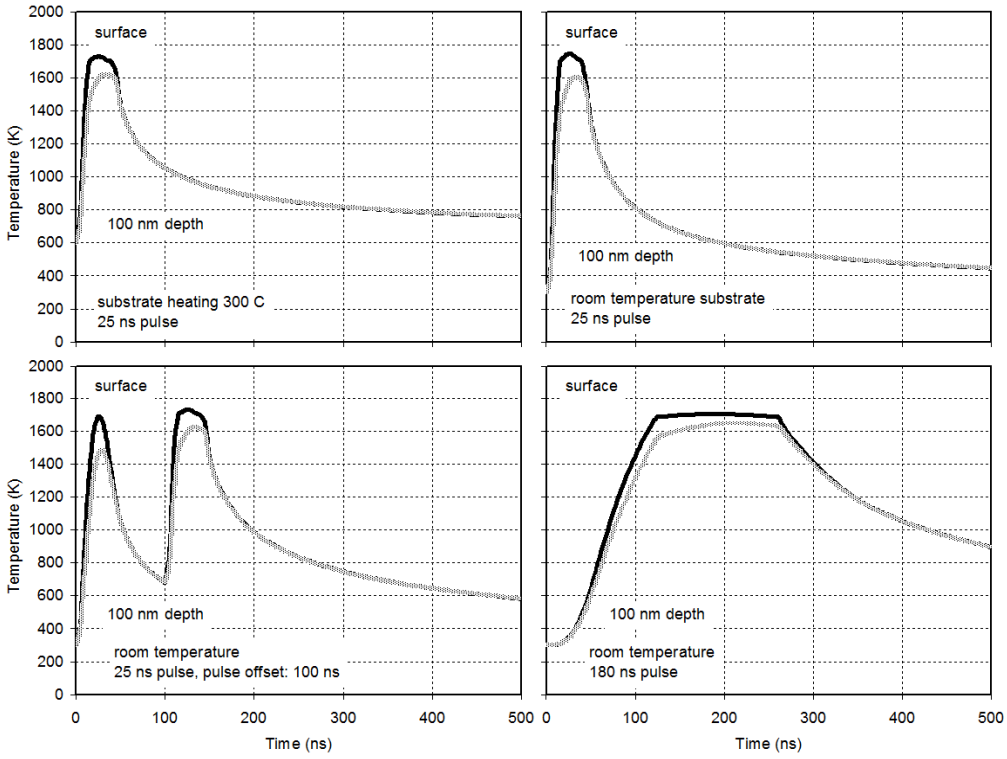

Fig.4. Calculated temporal thermal profiles at the silicon surface and at 100 nm depth for the different laser anneals.

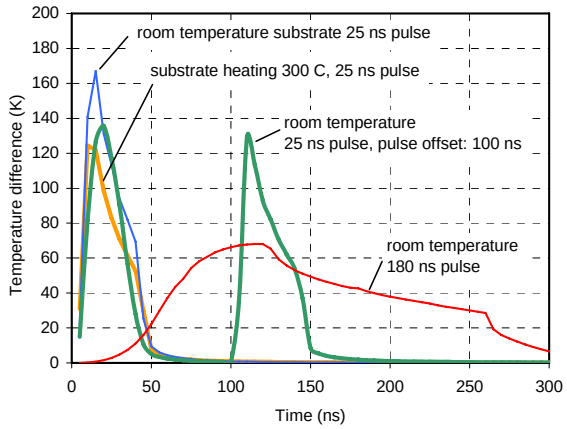

Fig. 5. Temperature difference between 50 and 100 nm depth as a function of time for the different laser anneals.

4. Conclusions

Various ultra short surface annealing thermal cycles were realized by double pulsed excimer laser annealing and long pulse excimer laser annealing. Full-melt energies can range from 600 to 1850 mJ/cm^2 were determined for on arsenic implanted silicon at 15 keV, 5 x 10^{14} cm^{-2} to demonstrate dopant activation with different energy depend on the substrate heating, the pulse width and shape. These parameters will also determine the temporal and spatial thermal gradients, which were determined by simulations.

To fully anneal the implanted As^+, a 25 ns pulsed laser anneal at room temperature requires 800 mJ/cm^2 fluence, and provides the smallest heat affected zone. In double pulsed laser annealing, the heat pulse generated by the first laser pulse is longer than the delay between the laser pulses, therefore at short offsets the heat pulses are superposed. This way, thermal budget can be increased by 20-50% with the pulse offsets maintaining the melt depth. By using equal pulses at an offset of 100 ns, the first pulse heats, and the second pulse completes the activation, and the full activation can be reached at 600 mJ/cm^2/pulse. The thermal cycle of the second pulse resembles the cycle when the substrate was heated to 300 ^{o}C. Largest thermal budget can be realized with long pulse, which results in low thermal gradients, therefore large heat affected zone.

Acknowledgements

The authors would like to acknowledge the support from the Philips/NXP PACD project and the cooperation with the EU FP6 D-DOTFET project.

References

[1] G. Lorito, V. Gonda, S. Liu, T. L. M. Scholtes, H. Schellevis, L.K. Nanver, Proc. MIEL, IEEE, 369-372, 2006.
[2] G. Lorito, V. Gonda, T. L. M. Scholtes, L. K. Nanver, Proc. MIEL, IEEE, 291-294, 2008.
[3] C. Biasotto, V. Jovanovic, V. Gonda, J. van der Cingel, S. Milosavljevic, L. K. Nanver, Proc. IEEE-ULIS, **10**, 181 (2009). (Eds S. Mantl, M. Lemme, J. Schubert, W. Albrecht)
[4] V. Gonda, S. Liu, T.L.M. Scholtes, L. K. Nanver, in Doping Engineering for Device Fabrication, edited by B. J. Pawlak, S. B. Felch, K.S. Jones, M. Hane (Mater. Res. Soc. Symp. Proc. 912, Warrendale, PA), 2006.
[5] J. Venturini, M. Hernandez, D. Zahorski, G. Kerrien, T. Sarnet, D. Debarre, J. Boulmer, C. Laviron, M.-N. Semeria, D. Camel, J.-L. Santailler, Proc. Mat. Res. Soc. Symp. Proc., **765**(D7.3), 1-6 (2003).
[6] V. Gonda, PhD thesis, Delft University of Technology, 2008.
[7] V. Gonda, J. Slabbekoorn, L. K. Nanver, Proc. IEEE-RTP, **15**, 257 (2007).
[8] R. F. Wood, G. E. Jellison, Semiconductors and Semimetals **23**, 165 (1984).

*Corresponding author: gonda.viktor@mail.duf.hu